Microstructural evolution of tool steels after Nd-YAG laser repair welding

M. VEDANI
Politecnico di Milano—Dipartimento di Meccanica, Via La Masa, 34, I-20158 Milano, Italy
E-mail: maurizio.vedani@polimi.it

The present paper is aimed at investigating the microstructural behaviour of tool steels after repair welding or refurbishing by a pulsed Nd-YAG precision laser. The 1.2311 (40CrMnMo7), 1.2083 (X42Cr13) and 1.2343 (X38CrMoV5-1) steels were selected for experimental investigations to cover a wide range of steel grades, commonly used in tooling industry.

Laser repair welding condition was simulated by preparing small deposits in one or more passes on steel samples having several reference geometries. Investigations on microstructural properties, microhardness evolution and on defect formation were carried out. The effects of different laser welding parameters were also considered.

The study allowed to state several fundamental information on tool behaviour during repair welding in order to gain a deeper insight into this process, routinely considered in industrial practice but often neglected in scientific research works on welding metallurgy.

1. Introduction

A large part of tool steels is commonly considered as critical in welding or even non weldable. Despite this statement, processes based on fusion welding are frequently adopted for production of tool assemblies, for deposition of hard and wear resistant overlays, for rebuilding worn or cracked surfaces and to modify the shape of existing tools. In particular, repair welding and refurbishing on dies are routinely performed to remove the traces of heat checking, surface wear, erosion and stress cracking, thus increasing significantly the tool life [1].

The most common process currently in use is gas tungsten arc welding (GTAW) owing to great process control suited for small areas, thin sections and sharp edges. According to industrial practice, repairing of the tool is done by first removing the damaged parts by milling or grinding and by rebuilding the missing volume by welding with a suitable filler metal. Pre-heating and post-weld heat treating are generally carried out to avoid solidification cracking and excessive residual stresses induced by welding [2, 3].

For distortion sensitive tools, high-density heat input processes such as electron beam and laser beam welding are preferred. The lower net heat input required to produce the weld reduces part distortion and allows the repair of thermally sensitive steel grades without additional pre- and post weld thermal treatments. Laser welding is particularly appreciated owing to the exact positioning and focalisation control of the beam that allows elevated accessibility even in thin and narrow areas that cannot be welded conventionally [4]. Especially, pulsed laser welding is receiving a great attention as a welding process of great precision and flexibility. Academic and industrial research efforts are mainly focussed on application of precision welding requiring extremely low thermal loads, narrow seam and elevated welding speed [5, 6]. The outstanding process flexibility of lasers applied to the tooling field was recently demonstrated in research works by Ernst and co-workers [4] and by Ben-Salah and Krauss [7]. These authors clearly highlighted the potential of laser refurbishing, cladding and caving as well as possible metallurgical transformations induced by laser processing on tool steels.

Several papers were also published on fundamental issues about process optimisation of pulsed laser welding. Especially, pulse shape effects were carefully studied by numerical models and by experimental investigations for defect prevention, microstructure optimisation and enhancement of productivity for a large variety of steel grades [8–14]. However, from a thorough literature survey, it appears that a deep knowledge on the microstructural aspect of pulsed laser tool steel welds is not fully achieved. A contribution to fill this lack of literature data is given by the present paper. An experimental investigation on microstructural behaviour of tool steels after repair welding by a Nd-YAG precision laser is described. Laser refurbishing was simulated by preparing small deposits in one or more passes on steel samples having several reference geometries. Analyses on microstructure, microhardness evolution and defect formation are described in the present paper.

TABLE I Nd-YAG laser processing parameters

	STD	HP	HF
Pulse frequency (Hz)	9.5	9.5	15
Pulse duration (ms)	6	6	4.5
Avg. pulse power (kW)	1.3	1.7	1.4
Spot diameter (mm)	0.8	0.8	0.8
Travel speed (cm/min)	9	9	9
Heat input rate[a] (J/cm)	494	646	630
Shielding gas	Argon	Argon	Argon

[a]a unitary absorption coefficient was considered.

TABLE II GTAW processing parameters

Current (A)	125
Voltage (V)	15
Polarity	DC, straight
Travel speed (cm/min)	10
Heat input rate (J/cm)	11250
Shielding gas	Argon
Diameter of *W* electrode (mm)	2.4
Arc gap (mm)	2.5

2. Materials and experimental procedures

The 1.2311 (40CrMnMo7), 1.2083 (X42Cr13) and 1.2343 (X38CrMoV5-1) tool steels were investigated to cover a wide range of grades, selected amongst those commonly used in tooling industry. Plates of the 1.2343 and 1.2083 steels were hardened and tempered to achieve final hardness values of 50 and 57 HRC, respectively, while the 1.2311 grade was studied in the annealed condition with a hardness of 29 HRC. Plates of the three steels (20 mm thickness) were prepared for the pulsed laser welding trials by accurate grinding of their parallel planes and by machining several grooves of 0.2 or 1 mm in depth and 10 mm in width to be filled by welding.

Refurbishment simulation was performed by using a Nd-YAG laser equipment (CRONITEX Vario Laser 9000). Table I summarizes the three different sets of welding parameters adopted. Standard laser processing conditions were first selected according to practical experience (parameters STD). Additional tests were performed by increasing the average peak power of the pulse (parameters HP) and by increasing the pulse frequency (parameters HF). In the table, an approximate assessment of the nominal heat input rate is given by combining the average peak power of the pulse, the pulse frequency and the welding speed. However, it must be specified that the actual heat transferred to the steel is strongly dependent on the absorption coefficient of the surface [15]. Suitable commercial filler wires of 0.4 mm in diameter were used to produce weld deposits by partially or totally filling the grooves machined in the plates. For the adopted laser system, feeding of the filler wire was performed manually. This technique provides large flexibility for operational welding at the expenses of possibly slight inhomogeneity in weld metal properties due to uneven feeding of the filler fire to the molten pool during welding.

Comparison tests were also carried out by GTAW welding the 1.2311 and 1.2343 steel grades. Suitable filler metal rods of 1.6 mm in diameter were used for this purpose. For all the welding techniques and base metals, the deposits were produced without any pre- and post-weld heat treatment. Table II supplies the main welding parameters adopted for GTAW welding.

In Table III data on chemical composition of the parent steels and of the filler wires are supplied. Due to the small diameter of the wires, chemical analysis of the filler metals were performed by a electron probe microanalysis (EPMA) system linked to a scanning electron microscope (SEM) while data about the parent metals were obtained by a spark emission spectrometer.

After welding, the plates were rough sectioned by abrasive water jet cutting. Metallographic samples were collected by further cutting with a precision diamond blade saw transversally to the weld deposits and prepared by conventional grinding, polishing and etching procedures. The prepared samples were microstructurally investigated by optical and scanning electron microscopy. Microhardness profiles in the different regions of the welds were generated by using a Vickers microhardness tester with a load on the indenter of 50 g.

3. Results and discussion

3.1. Macroscopic aspect of the deposits

In Fig. 1 representative macroscopic views of Nd-YAG laser and GTAW deposits are shown. The comparison

TABLE III Chemical composition (mass%) of the parent metals, of the filler wires and of the resulting weld metals obtained by the STD Nd-YAG laser welds and by the GTA welds

	C	Si	Mn	Cr	Ni	Mo	Cu	V
1.2311 parent metal	0.44	0.40	1.38	1.83	0.38	0.17	0.19	
Filler wire for 1.2311 laser[a]	–	0.69	1.06	1.26	0.06	0.64	0.03	
1.2311 laser weld metal[a]	–	0.67	0.86	1.31	0.12	0.58	0.08	
Filler wire for 1.2311 GTAW[a]	–	0.72	1.02	1.33	0.09	0.62	0.41	
1.2311 GTA weld metal[a]	–	0.59	1.18	1.77	0.26	0.30	0.27	
1.2083 parent metal	0.36	0.77	0.51	14.46	0.18	0.01	0.14	
Filler wire for 1.2083 laser[a]	–	0.69	0.48	6.15	0.12	0.61	0.10	
1.2083 laser weld metal[a]	–	0.73	0.38	8.87	0.19	0.54	0.10	
1.2343 parent metal	0.43	0.91	0.43	4.97	0.03	1.24	0.20	0.37
Filler wire for 1.2343 laser[a]	–	0.69	0.42	6.10	0.12	0.61	0.10	0.02
1.2343 laser weld metal[a]	–	0.91	0.29	5.57	0.06	1.06	0.09	0.12
Filler wire for 1.2343 GTAW[a]	–	1.51	0.47	6.58	0.34	2.00	1.41	0.22
1.2343 GTA weld metal[a]	–	1.06	0.42	5.40	0.32	1.64	0.40	0.39

[a]measured by EPMA.

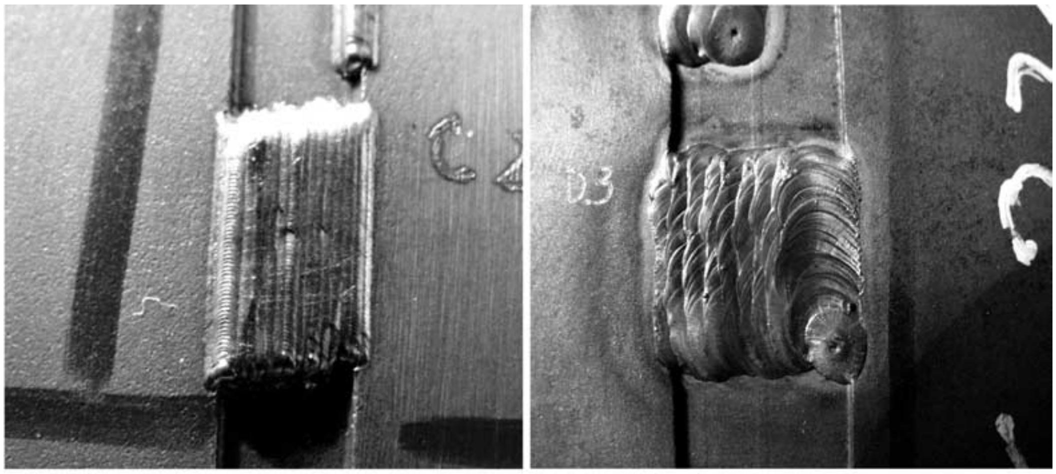

Figure 1 Macroscopic views of the welds: (a) multipass Nd-YAG deposit, (b) multipass GTAW deposit. Groove width corresponds in both cases to 10 mm.

with the GTAW deposits clearly emphasizes the reduced size of the laser processed deposits and the improved surfacial homogeneity. For all of the materials and laser process parameters considered, it was apparent that appropriate deposition and solidification conditions were achieved, leading to smooth, geometrically regular and macroscopically defect-free weld beads. Such features suggest the possibility of exploiting Nd-YAG laser for near net shape refurbishment of steel dies.

3.2. Microstructure of single pass welds

In Fig. 2 cross-sectional views of the single pass laser welds performed on the 0.2 mm deep groves are depicted. The effect of the pulsed heat input is clearly emphasised in Fig. 2a through 2c by the heterogeneous weld metal structure and by some irregularities of the fusion line shape (especially in the 1.2083 steel grade weld). A contribution to macroscopic perturbations of the weld pool shape is believed to be promoted by the manual feeding of the filler wire as well.

Occasional defects based on incomplete fusion phenomena within the weld metal zone were also noted (see Fig. 2a and c). The above weld discontinuities were accounted for by local variations of the heat input rate due to the pulsed heat source, leading to abrupt interruption of the solidification front followed by a sudden restart of solidification with insufficient liquid metal feeding [14].

It is worth mentioning that difficulties were encountered to achieve an appropriate etching of the laser weld metal structure by conventional metallographic reagents. Similar comments were already known from literature whereby specific rapidly solidified metal structures (e.g., wire electro-discharge machined surface layers) appear as featureless on metallographic analyses [16]. After optimised etching time, the fine weld metal structure could be satisfactorily resolved, at least in some regions of the weld beads. Figs 3 and 4 show two examples of the weld metal structure found in the materials investigated. In Fig. 3 the typical structure of the 1.2311 steel is depicted. In the upper part of the micrograph a martensitic structure is observed together with relevant amounts of residual austenite. The lower part of the micrograph is separated from the former by a region where partial lack of adhesion of two solidification fronts occurred. The underlying structure fairly resembles that found in multipass welds, featuring well visible tempering phenomena and conversion of residual austenite in the root passes. In the present case, microstructural modifications similar to those generated by multipass welding were supposed to be due to the pulsed effects of the laser source, inducing interruptions and accelerations of the solidification front on a short time scale.

Fig. 4 shows a higher magnification SEM image of the weld metal zone of the 1.2343 steel grade. The original solidification structure is made up of tiny elongated cells having an average size of the order of 2 μm. As expected, after rapid cooling, a martensitic structure formed in the weld metal.

In Table III, the chemical compositions of the weld metals, as measured by EPMA at centre of the weld metal regions, were also given. It is apparent from the data that the alloying element content of the weld metal is the result of dilution effects of the filler wire and of the parent metal. Apart from some occasional discrepancies related to intrinsic lack of precision of the microanalysis system, it can be generally stated that the dilution effect of the filler alloy by the parent metal was less important in the laser welds as compared to GTA welds, as expected.

Microstructural observations on heat affected zone (HAZ) structures allowed to demonstrate that significant modifications were limited to less than 100 micrometers for the 1.2311 and 1.2343 steel grades and to less than 200 micrometers for the 1.2083 steel grade (see Fig. 2). In Figs 5 and 6 more detailed views of the high-temperature HAZ of the 1.2083 and 1.2343 steels are reported. The thermal modification close to the weld metal region, within a layer of the order of a few micrometers from the fusion line, consisted of the re-austenitisation of the steels as well as dissolution of Cr-rich carbides in the 1.2083 grade due to high peak-temperature reached, followed by martensite formation on rapid cooling. Concerning this aspect, it is

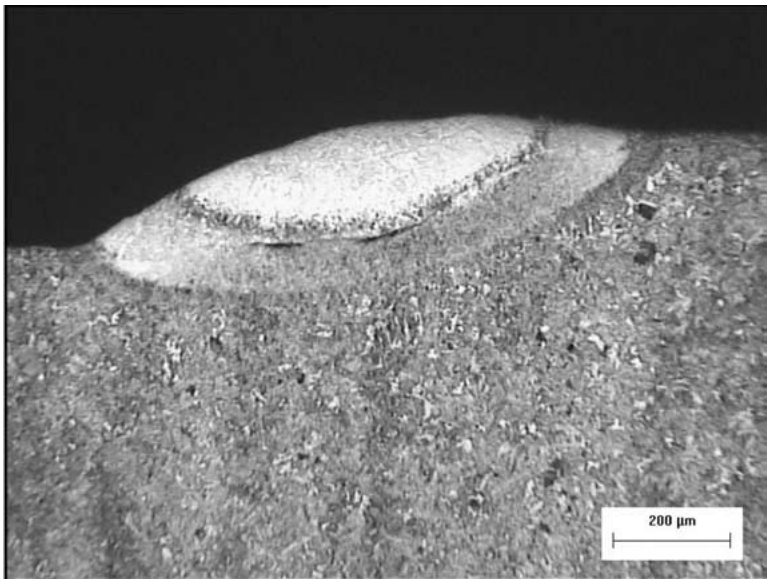

(a)

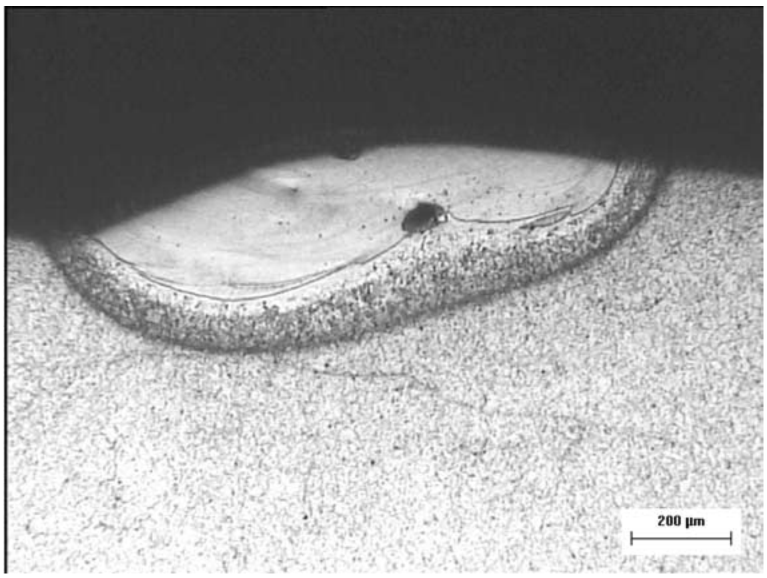

(b)

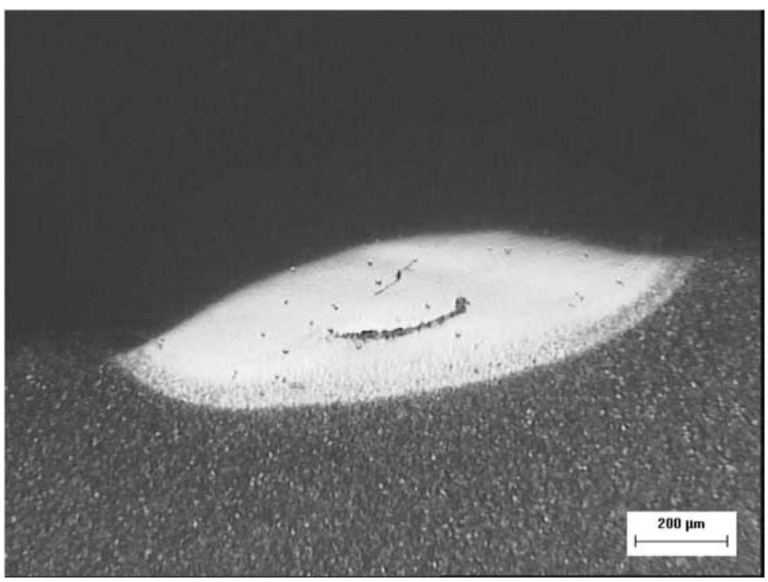

(c)

Figure 2 Optical micrographs of the single-pass laser welds: (a) 1.2311 grade, (b) 1.2083 grade, and (c) 1.2343 grade.

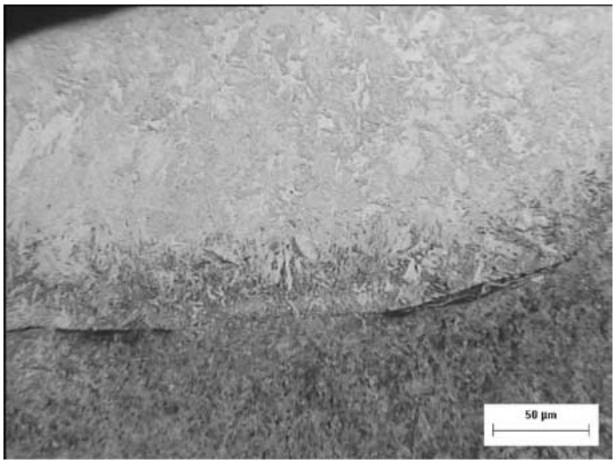

Figure 3 Microstructure of single-pass laser weld metal region of the 1.2311 steel grade.

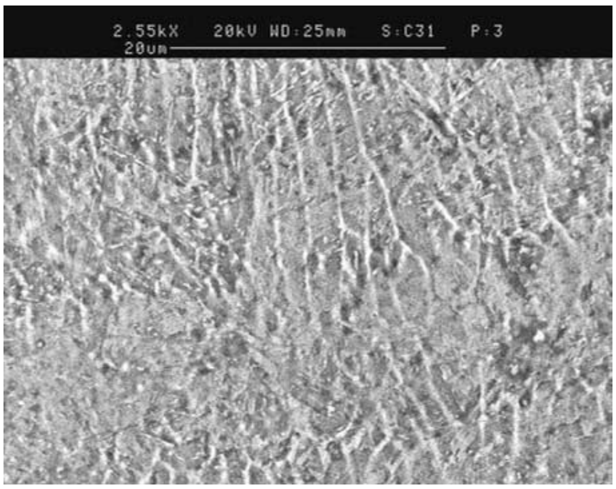

Figure 4 Microstructure of single-pass laser weld metal region of the 1.2343 steel grade.

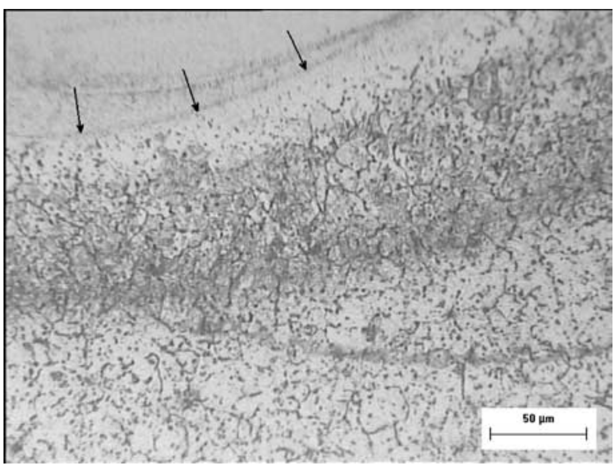

Figure 5 Microstructure of single-pass laser weld HAZ of the 1.2083 steel grade. Arrows indicate the fusion line location.

worth mentioning that, in the absence of post-weld heat treatment, there is no means to relieve residual stresses and brittleness of this fully martensitic region. Therefore, it often defines the integrity and durability under service of the entire weld.

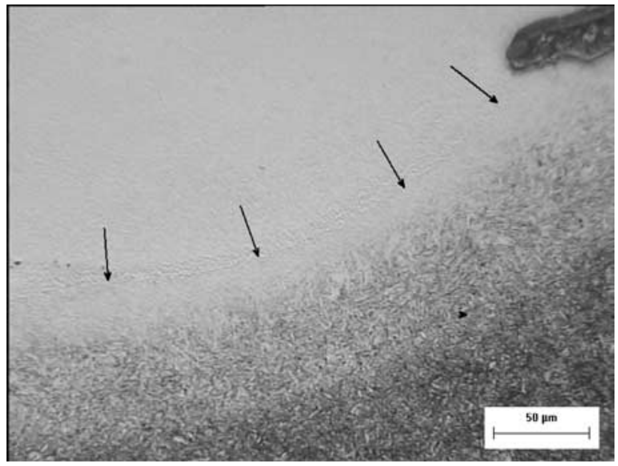

Figure 6 Microstructure of single-pass laser weld HAZ of the 1.2343 steel grade. Arrows indicate the fusion line location.

When moving away from the fusion line, the low-temperature HAZ is encountered, where overtempering effects are clearly visible also on low magnification micrographs (see Fig. 2b). It is worth mentioning that in the upper right corner of Fig. 5 an occasional coarse oxide inclusion is also visible.

The reference single pass welds produced by the GTAW procedure featured significantly larger weld bead volume and HAZ. Structural modifications in the latter zone, detectable at the optical or SEM microscopes, extended for about 1 mm from the fusion line toward the parent metal. Fig. 7 depicts a representative micrograph of the GTAW weld microstructure of the 1.2343 grade. For both steels investigated under GTAW welding conditions, a equiaxed grain structure was initially detected in a thin layer adjacent to the fusion line and it was soon replaced by a cellular structure oriented according to heat extraction flow pattern. The average cell size in the central weld metal region was of the order of 10 μm.

3.3. Microstructure of multipass welds

Multipass deposits were produced to investigate the effects of the repeated welding thermal cycles on parent metal structure and to evaluate the multipass weld integrity. In Fig. 8 macroviews of the multipass deposits performed under standard laser parameters for the different steels are gathered whereas in Fig. 9 the effects of different welding parameters for the 1.2343 steel grade are shown.

A notable microstructural heterogeneity is observed within the weld metal zones as a consequence of the combined effects of multipass metal deposition procedure and of the pulsed laser action within a single pass. It is also apparent from optical and SEM micrographs that the root pass microstructure is not significantly altered by the subsequent passes performed to complete the deposits. In addition, the HAZ extension observed on optical micrographs is comparable to that found for the single pass deposits (compare Fig. 8 to Fig. 2). Lack of penetration at the lower edge of the machined grooves were found in several deposits (see Fig. 8a and

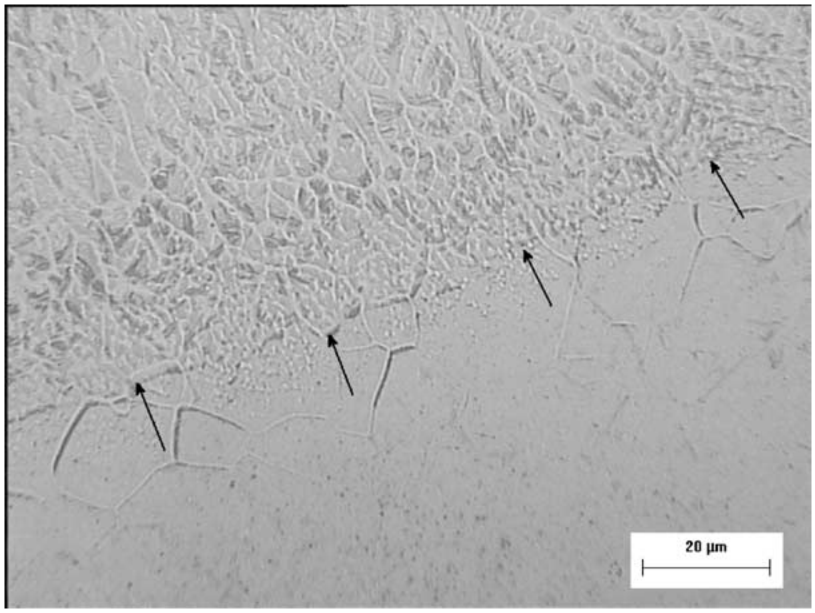

Figure 7 Microstructure of the 1.2343 steel GTAW fusion line region. Arrows indicate the fusion line location.

c). In addition, oxide inclusions and micropores were also observed in some deposits.

As far as the effects of laser parameters on multipass deposits are concerned, from the present data it is suggested that the imposed welding conditions did not induce remarkable modifications of the weld bead morphology or of the defect population. The slight changes of the weld bead profiles observed in Figs 8 and 9 are believed to be mainly due to irregularities related to manual feeding of the filler wire.

3.4. Microhardness

In Fig. 10 the microhardness profiles of the 1.2311 steel grade under single pass and multipass deposition conditions are depicted. Microhardness evolution was measured along vertical lines starting from the top surface of the deposit and moving across the weld metal zone toward the HAZ and the unaffected parent metal. From a comparison between Fig. 10a and the corresponding weld microstructure given in Fig. 2a it is inferred that the structural modifications visible as darker (more reactive to etchant) regions within the weld metal are strictly related to the peaks visible in the microhardness profiles, the peaks immediately preceding the darker regions. A similar relation also holds for the multipass deposits. It was also observed that the average hardness values measured in the weld metal multipass samples were significantly lower than those of the single pass deposits. It is supposed that stress relieving effects as well as tempering of the martensite occurs when passes are overlaid on the pre-existing deposit.

Finally, in Fig. 11 the microhardness profiles of the manual GTAW deposits are given. Also for the GTAW welds, hardness fluctuations due to process alterations are observed, particularly for the 2311 steel grade. A high hardness HAZ is observed in both graphs having a width of 0.8 and 1.2 mm for the 1.2311 and 1.2343 steel, respectively. For the hardened and tempered 1.2343 grade, a further low hardness HAZ is observed extending for about 1 mm.

4. Conclusions

The experimental investigation on pulsed Nd-YAG laser repair welding allowed to draw the following conclusions related to microstructural modifications of the tool steels.

1. Weld deposits produced by partially or totally filling machined grooves on tool steel samples had a homogeneous and defect free surface aspect. Improved weld bead geometry control over the reference GTAW welds was achieved by the use of a precision laser having a pulsed Nd-YAG heat source.
2. From analyses on cross sectioned weld samples produced by single pass or multipass conditions, it was observed that a heterogeneous weld metal structure developed due to laser pulse effects and manual feeding of filler metal, inducing local fluctuations of the solidification conditions. Defects based on incomplete fusion at the fusion line and within the weld metal were detected.
3. Microhardness profiles measured across the weld deposits showed that the above described microstructural alterations corresponded to changes in mechanical behaviour as well. In the single pass laser and GTAW welds, high hardness values were measured, consistently with the fully martensitic structure obtained in the weld metal zone. In multipass laser deposits, significantly lower microhardness values were measured due to stress relieving and tempering effects of the martensite by subsequent passes.
4. As expected, the weld metal regions generated by Nd-YAG laser processing had a significantly finer structure with respect to the GTAW welded materials. In the 1.2343 steel grade a cellular structure was observed in both cases, their size being 2 and 10 μm for the laser and GTAW weld metal, respectively.

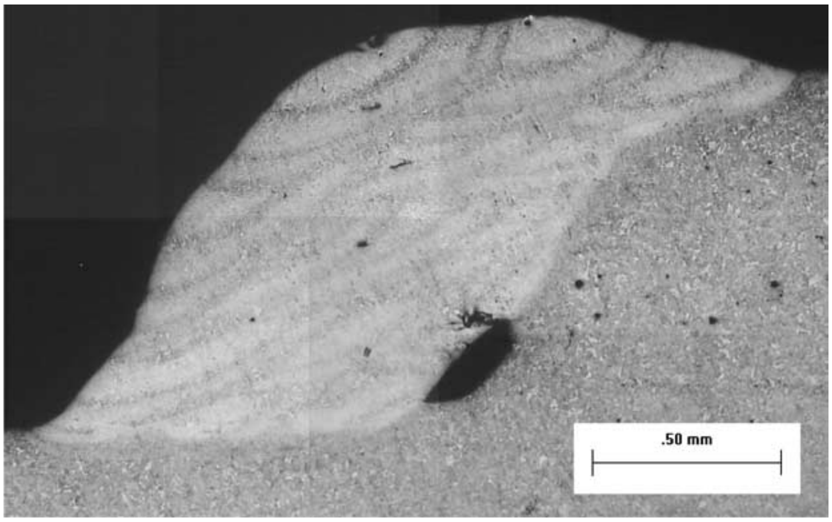

(a)

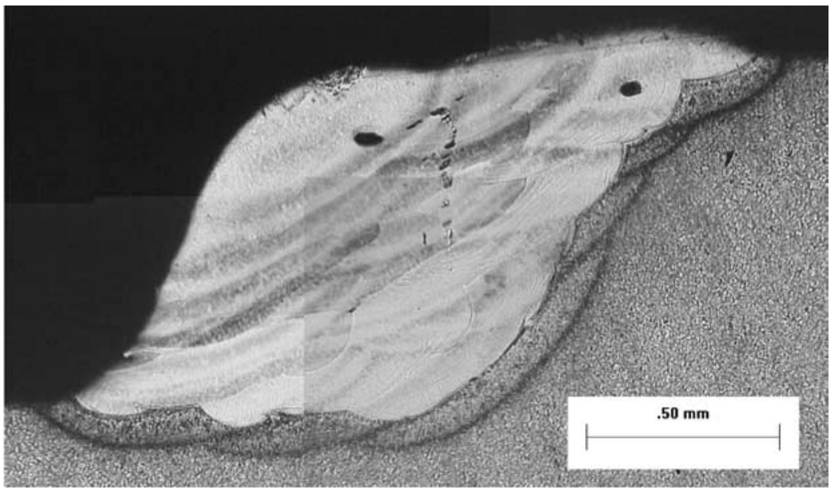

(b)

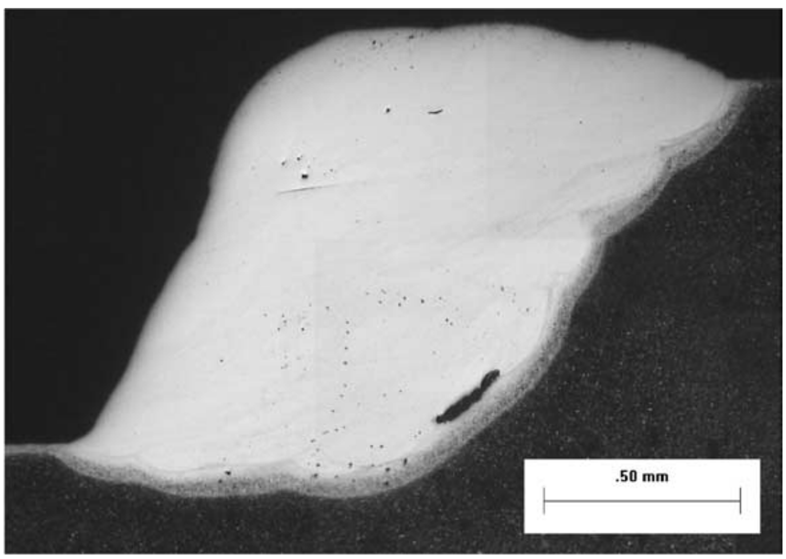

(c)

Figure 8 Microstructure of Nd-YAG multipass welds performed by standard parameters: (a) 1.2311 steel, (b) 1.2083 steel, and (c) 1.2343 steel.

5. Information on HAZ extension were obtained both from microstructure and microhardness data. The laser processed steels featured a narrow high-temperature HAZ where the structure reconverted to austenite and the carbides dissolved during the heating phase of the thermal welding cycles. On subsequent rapid cooling to room temperature, a high-hardness fully martensitic region of about 20 μm in width formed. Similar phenomena were also noticed in the GTAW deposits but the HAZ extension was

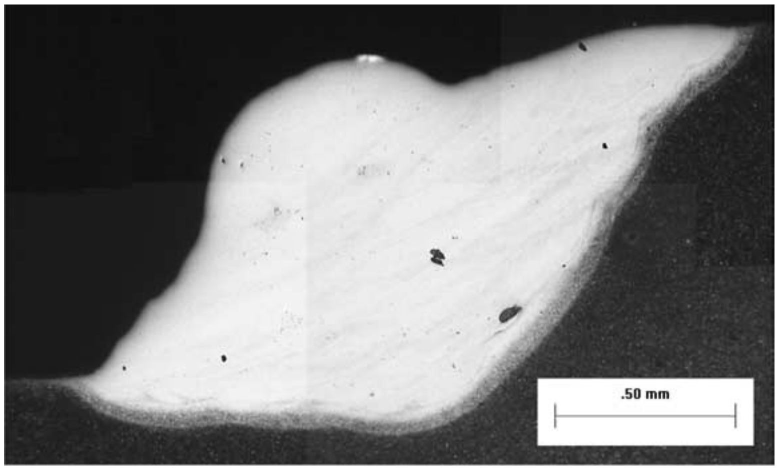

(a)

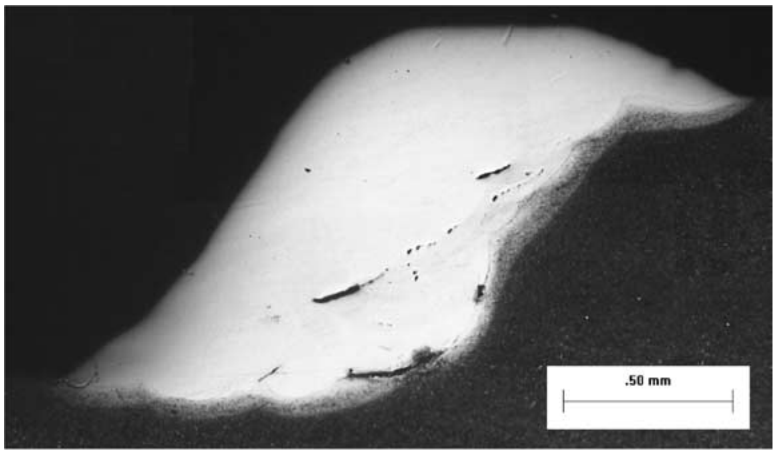

(b)

Figure 9 Microstructure of 1.2343 Nd-YAG multipass welds performed by (a) high pulse power and (b) high pulse frequency parameters.

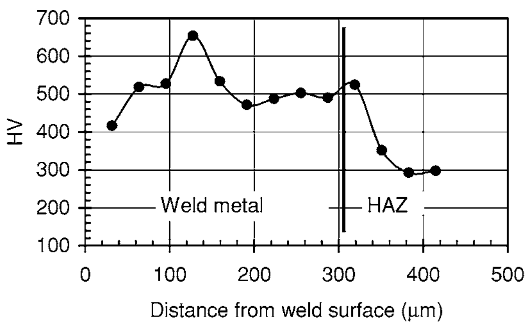

(a)

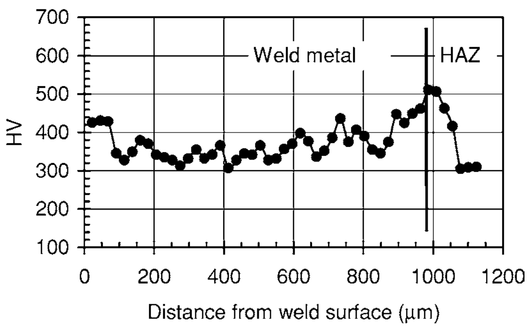

(b)

Figure 10 Microhardness profiles across the laser deposits of the 1.2311 steel grade: (a) single pass deposit and (b) multipass deposit.

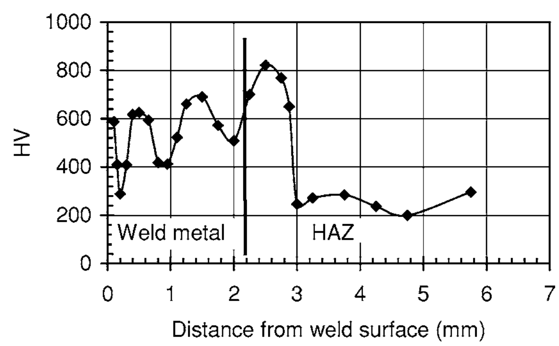

(a)

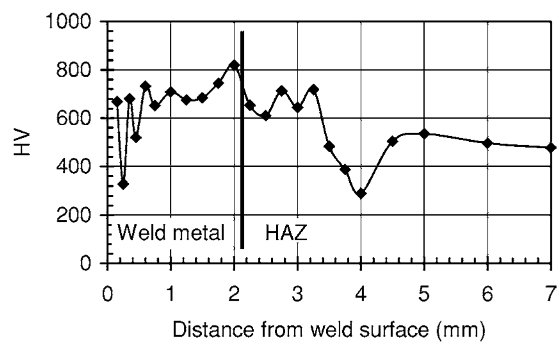

(b)

Figure 11 Microhardness profiles across the single pass GTAW deposits: (a) 1.2311 grade and (b) 1.2343 grade.

comparatively much larger, the high-hardness HAZ region width being 0.8 and 1.2 mm for the 1.2311 and 1.2343 steel grades, respectively.

Acknowledgements

The author would like to thank Mr A. Moriggi (F.lli Moriggi SrL, Cormano—Italy) for preparing the welded samples and for the helpful discussions of the results. The experimental work carried out by Dr. G. Fasoli and Dr. M. Rinaldi is also greatly appreciated.

References

1. Welding and Brazing of Tool Steels, in "ASM Metals Handbook" (ASM, 1990) Vol. 6.
2. J. BRUHAGEN, in Proceedings of the Fifth International Conference on Tooling, Leoben, 1999, edited by F. Jeglitsch, R. Ebner and H. Leitner (1999) p. 463.
3. A. HENZE, H. HAFERKAMP and M. NIEMEYER, F.-W. BACH, in Proceedings of the Fifth International Conference on Tooling, Leoben, 1999, edited by F. Jeglitsch, R. Ebner and H. Leitner (1999) p. 453.
4. G. ERNST, A. LUFTENEGGER and R. EBNER, in Proceedings of the Fifth International Conference on Tooling, Leoben, 1999, edited by F. Jeglitsch, R. Ebner and H. Leitner (1999) p. 437.
5. A. JURASCHIK, U. SCHIEGG and R. MAYERHOFER, *Ind. Laser Solutions* **5** (2001) 26.
6. Y. SUN, H. SUNADA and N. TSUJII, *ISIJ Int.* **41**(9) (2001) 1006.
7. N. BEN-SALAH and G. KRAUSS, in Proceedings of the Fifth International Conference on Tooling, Leoben, 1999, edited by F. Jeglitsch, R. Ebner and H. Leitner (1999) p. 307.
8. S. KATAYAMA, S. KOHSAKA, M. MIZUTANI, K. NISHIZAWA and A. MATSUNAWA, in Proceedings of International Conference: ICALEO'93–Laser Materials Processing, Orlando FL, 1993 (1994) p. 487.
9. J. GRIEBSCH, P. BERGER, F. DAUSINGER and H. HUGEL, in Proceedings of International Conference: ICALEO'94—Laser Materials Processing, Orlando FL, 1994, edited by T. D. McCay, A. Matsunawa and H. Hugel (1994) p. 173.
10. S. KATAYAMA, T. TAKEMOTO and A. MATSUNAWA, in Proceedings of International Conference: ICALEO'95—Laser Materials Processing, San Diego, CA, 1995, edited by J. Mazumder, A. Matsunawa, C. Magnusson (1995) p. 846.
11. M. R. FREWIN and D. A. SCOTT, in Proceedings of International Conference: ICALEO'95—Laser Materials Processing, San Diego, CA, 1995, edited by J. Mazumder, A. Matsunawa and C. Magnusson (1995) p. 904.
12. H. N. BRANSCH, D. C. WECKMAN and H. W.KERR, *Welding J.* **6** (1994) 141-s
13. M. FREWIN, D. DUNNE and A. SCOTT *Sci. Techn. Weld. Joining* **3** (1998) 145.
14. Y.-F. TZENG, *J. Mater. Proc. Techn.* **100** (2001) 163.
15. R. W. MESSLER, in "Principles of Welding—Processes, Physics, Chemistry and Metallurgy" (J. Wiley & Sons, New York, 1999) p. 260.
16. L. C. LIM, L. C. LEE, Y. S. WONG and H. H. LU, *Mater. Sci. Techn.* **7**(3) (1991) 239.

Received 15 July 2002
and accepted 14 August 2003